

PRESENT PUZZLES OF ENTANGLED POLYMERS

Tom C. B. McLeish

**Department of Physics and Astronomy
University of Leeds, Leeds LS2 9JT, UK**

ABSTRACT

Entangled polymeric fluids, including high molecular weight polymer melts, constitute a fundamental example of viscoelastic fluids. In spite of enormous advances in understanding the molecular origin of their rheology and microscopic dynamics, there are several pressing puzzles, some of them strongly linked, that offer current and pressing challenges. We review the current state of the field and nature of five current challenges.

KEYWORDS: Molecular rheology; Tube model; Viscoelasticity; Branched polymers; Entanglements; Constraint release.

1. INTRODUCTION

The fascinating rheology of fluids containing flexible polymers flows from both necessity and beauty. Born of the rapid growth in synthetic polymer materials in the post-war years, the need to understand and control the processing of such highly viscoelastic liquids as polymer melts led rapidly to the fundamental investigations of Flory [1], Stockmayer [2] and Edwards [3]. These in turn were building on work of Kuhn [4] (how large would macromolecules, linear or branched, be?), and Zimm [5] and Rouse [6] (how would such giant molecules move?). These pioneers were already using a beautiful notion that was to take hold of condensed-matter physics in the mid 20th century - that of *universality*, or the independence of physical phenomena from local, small-scale details. The emergence of universal properties is usually associated with “critical phenomena” [7], since near phase transitions, the spatial scale of correlated fluctuations may hugely exceed molecular dimensions. Properties that depend on these fluctuations, such as compressibility of a fluid near its critical point, are then insensitive to molecular detail. Although there is at first glance no apparent neighbouring critical point in the case of polymeric fluids, both universality in exponents and renormalised quantities appear in abundance. Moreover, there is a natural large number associated with mesoscopic, rather than microscopic length-scales. The defining feature of a polymer is, after all, its large “degree of polymerisation”, N , the number of monomers linked together covalently to form the polymer chain. (The literature discusses interchangeably N and the *molecular weight* M of the chains, given in terms of the monomer molecular weight m_0 by $M = Nm_0$.)

Such an approach has been particularly effective in the realm of *topological* effects. The polymer melts of industrial polymer processing are very highly overlapped on the molecular level, where it becomes immediately apparent that molecular relaxation processes controlling elastic stress are prolonged to very long times indeed. The classic “relaxation modulus” $G(t)$ measuring stress linear-response to a step strain records a “plateau” value before a terminal relaxation time that increases rapidly with molecular weight. Experiments restricted to the timescales of the plateau are hardly able to distinguish between the polymer melt and a rubber, in which the chains are permanently cross-linked to each other at very rare points, sufficiently for each chain to be permanently immobilised from large-scale diffusion. Conceptually, the absent “cross-links” were replaced in the minds of engineers and physicists alike by “entanglements” [8]. These loosely-defined objects were assumed to represent the topological constraint that covalently-bonded molecular chains may not pass through each other. The effective distance between these objects could be calculated, employing rubber elasticity theory,

$$G_N^{(0)} = k_G \frac{RT\rho}{M_e},$$

(with the constant $k_G = 1$ for “affine” and $1/2$ for “junction fluctuation” models of elasticity) to deduce the degree of polymerisation between entanglements N_e , or the equivalent “entanglement molecular weight”, M_e . The number N_e consistently turned out to be of order 10^2 , indicating a length-scale for an “entanglement spacing” of 50-100 Å, depending on the particular chemistry. This is highly significant for us, because it shows that small chains on the threshold of feeling topological interactions are real polymers, already long enough to show to a good approximation all the universal properties of statistical connected chains. It also suggests that the role of topology in highly-entangled ($N \gg N_e$) polymer fluids has the potential to be treated universally. Further evidence of universality in entanglements came from experiments in which the polymers were diluted to a volume fraction ϕ_p by a compatible solvent. The apparent entanglement molecular weight $M_e \sim \phi_p^{-\alpha}$ where the scaling exponent $\alpha \equiv 1$ [9].

Other experiments had pointed to the existence of a topological feature at this coarse-grained scale of structure. Careful measurements on rubbers of controlled synthesis had shown that the shear modulus was higher for a network of long chains than a model incorporating cross-links alone would predict [10]. Other “trapped entanglements” on the same scale as the melt value of N_e seemed to contribute to the elasticity. Advanced theories of rubber elasticity have been able to treat rubber networks in terms of the two distinct constraints of physical cross-links and trapped entanglements [11,12]. A remarkable universality also emerged in measurements of the scaling of melt viscosity η on the molecular M of very many different polymer chemistries [8]:

$$\begin{aligned} \eta &\sim M^1 & M < M_c & . & \dots\dots\dots(1) \\ \eta &\sim M^{3.4} & M > M_c & \end{aligned}$$

For each material, a critical molecular weight, M_c emerged, above which the viscosity rises very steeply with molecular weight. Moreover, within experimental error, this explicitly dynamical observation was linked phenomenologically to the essentially static measurements of the plateau modulus by the correlation:

$$M_c \cong 2M_e. \quad \dots\dots\dots(2)$$

This connection between essentially dynamic (M_c) and static (M_e) experiments, observed over a wide range of chemistries, is strong evidence that topological interactions dominate both the molecular dynamics and the viscoelasticity at the 10nm scale in polymer melts (and at correspondingly larger scales for concentrated solutions).

Without going beyond rheological measurements on bulk samples, there has long been other very strong evidence that molecular topology is the dominant physics in melt dynamics. This emerges from the phenomenology of “long chain branched” (LCB) melts. These materials, commonly used in industry, possess identical molecular structure to their linear cousins on the local scale, but contain rare molecular branches. The density of branching varies from one branched carbon in every 10,000 to 1 in 1000. This level is chemically all but undetectable, yet the melt rheology is changed out of all recognition if the molecular weight is high enough [13]. Providing that $M \gg M_c$, the limiting low-shear viscosity may be much higher for the same molecular weight. Moreover in strong extensional flows the melt responds with a much higher apparent viscosity than in linear response. This phenomenon, vital for the stable processing properties of branched melts, is called “extension hardening”. The effect is all the more remarkable because in shear flows, branched, as well as linear, melts exhibit a lower stress than would be predicted by a continuation of their linear response [14] (they are “shear-thinning”). A fascinating example of the difference between linear and branched entangled melts is well-known from flow-visualisation experiments. The velocity field in a strong “contraction flow” of a linear polymer melt resembles that of a Newtonian fluid, while that of a branched polymer sets up large vortices situated in the corners of the flow field. Slight changes to the topology of the molecules themselves give rise to qualitatively different features in the macroscopic fluid response.

Theoretical treatments of the “dynamical slowing down” beyond the entanglement scale have fallen into two classes. The first treat the physics as collective effects, without seeking to capture the topological nature of constraints explicitly. Starting with the Rouse theory, collective corrections introduced to the monomer mobility lead both to slowing down and to local anisotropy. An example is the approach of Williams and co-workers [15]. The second approach treats the entanglements phenomenologically, but as serious topological constraints. The most successful of these has been the *tube model*. The idea is to deploy the theoretical physicists favourite strategy of replacing a difficult many-body problem with a tractable single-body problem in an effective field. In this case the “single body” is the single polymer chain, and the effective field becomes a tube-like region of constraint along the contour of the chain. The tube is invoked to represent the sum of all topological non-crossing constraints active with neighbouring chains, and the tube radius, a , is of the order of the end-to-end length of a chain of molecular weight M_c . In

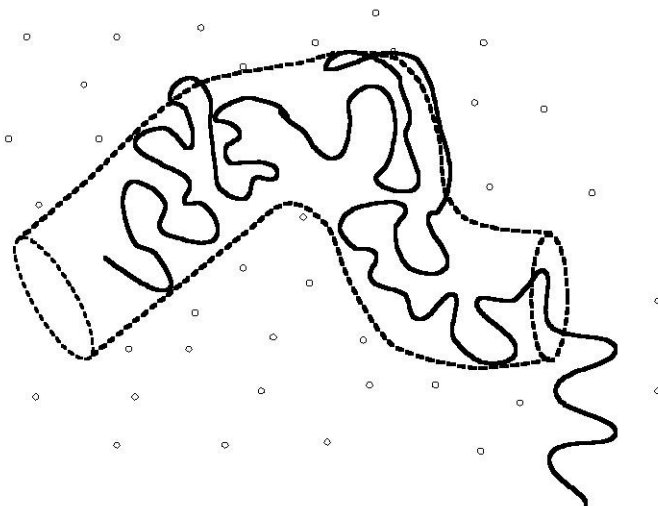


Figure 1: A tube-like region of constraint arises around any selected polymer chain in a melt due to the topological constraints of other chains (small circles) in its neighborhood (diagram courtesy of R. Blackwell).

this way, only chains of higher molecular weight than M_e are strongly affected by the topological constraints (see figure 1).

The tube was first invoked by Edwards [16] in an early model for the trapped entanglements in a rubber network. The consequences of the idea for dynamics were first explored by de Gennes [17], again in the context of networks. A free chain in a network would be trapped by the tube of radius a defined by its own contour. This would suppress any motion perpendicular to the tube's local axis beyond a distance of a , but permit both local curvilinear chain motions and centre-of-mass diffusion along the tube. de Gennes coined the term “reptation” for this snake-like wriggling of the chain under Brownian motion. The theory gives immediately a characteristic timescale for disengagement from the tube by curvilinear centre-of-mass diffusion. This disengagement time τ_d is naturally proportional to the cube of the molecular weight of the trapped chain (this arises from combining the Fickian law of diffusive displacement of length L with time τ , $\tau \sim L^2$, recognising that path length $L \sim M$, with one extra power arising from the proportionality of the total drag on molecular weight). Very significantly, de Gennes also realised that a tube-like confining field would endow a dangling arm, fixed to the network at one end, or belonging to a star-shaped polymer in a network, with exponentially slow relaxations. In this topology reptation would be suppressed by the immobile branch point [18], and only

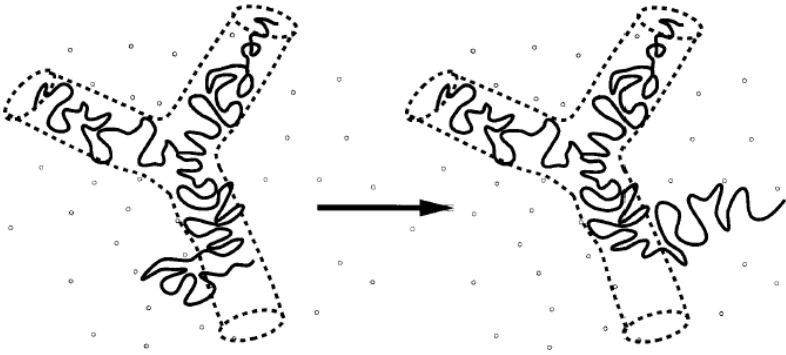


Figure 2: The process of arm retraction predicted by the tube model for the case of dangling entangled arms, as from the branch point of a star polymer. Unlike in reptation, reconfiguration of the outer parts of the arm occurs many times for one relaxation of deeper segments.

exponentially-rare retractions of the dangling arm would disengage it from its original tube (see figure 2).

In the late 1970s, S. F. Edwards and M. Doi developed the tube concept into a theory of entangled melt dynamics and rheology for monodisperse, linear chains [19]. The work rapidly caught the attention of the community for a number of reasons. The first was that the underlying idea is so simple. The tube-field is much easier to conceptualise, and the approximation much clearer than in approaches sometimes known as “mode-coupling”, in which the effective mean field is hidden in a dense forest of algebra. Secondly the tube-model made a parameter-free prediction for the most assessable non-linear function of strain - the so-called “damping function”. This is really an effective non-linear shear modulus as function of shear strain. The prediction was in very good agreement with available data. Thirdly, Doi and Edwards were able, by making a mathematical approximation they called the “independent alignment approximation” (IAA), to produce a *constitutive equation* in closed form of a recognisable type. Rheologists had since the 1940s sought these general mathematical forms relating the local stress tensor of a viscoelastic liquid to its local strain history. Relations were written down using both differential and integral forms, using notions of frame-invariance and algebraic simplicity to constrain the huge space of non-linear functionals that are possible [20]. The original Doi-Edwards formulation with the IAA took the form of an integral “K-BKZ” equation [21,22].

It is rather remarkable that the tube concept took such a hold in the following two decades in spite of some shortcomings of the early approximations that in retrospect are rather severe. The prediction that the viscosity $\eta \sim M^3$ rather than the observed $\eta \sim M^{3.4}$ was the mildest of them: in addition, the distribution of stress relaxation times in the response function $G(t)$ was much too sharp, and the prediction

for steady shear flow inherently unstable. In strong shear, the model had all the confining tubes align in the flow direction, forcing unstretched chains within them to do the same, so that eventually the shear stress would *reduce* with increasing shear rate. That polymer melts do indeed exhibit instabilities resembling slip-flow kept this idea alive for a while [23], but it is now clear that polymer melts do not possess this constitutive non-monotonicity of response. The original suggestions that the way to handle polydispersity in chain length would be a linear superposition of response was seen to fail strongly as soon as experiments on controlled bimodal blends were performed [24]. Finally, in early attempts to calculate the rheology of well-controlled star polymer melts, rather large *ad hoc* changes were required to the tube model's dimensionless constants [25]. All along there remained a concern over even the validity of the tube in melts, even if it were accepted in the case of permanent networks. After all, in the melt the tubes themselves arise from constraints imposed by other chains which are also reptating. During the lifetime of a tube segment, therefore, some of the surrounding chains will typically release their contributing constraints by bringing one of their free ends into the tube segment's volume. This issue of self-consistency via “constraint release” (CR) would require experiment, theory and simulation to sharpen.

Conceptual problems such as CR, and their relation to experimental observables, have meant that the last few years have seen very rapid progress across an increasingly broad canvas of research. These advances are changing the quality and pace of the field and need to be considered together, rather than in isolation, as real bridges are built between the fundamental physics of entangled polymer fluids and actual industrial practice. In this review article we first survey the new features that have contributed to this rapid period of development in section 2. Then we focus in a little more detail on a few selected current challenges in section 3.

2. THE PRESENT STATE OF THE FIELD

The first qualitative new feature is the explosive growth of experimental techniques able to probe polymer dynamics on the entanglement scale. No longer are we confined to the collective and macroscopic view of rheology, or even rheo-optical measurements [26, 27], but now have considerable accumulated data directly probing molecular motion. It is instructive to list the remarkable palette of techniques that the theoretician must now satisfy in making predictions:

1. Neutron spin-echo (NSE) [28, 29, 30] now permits dynamic and spatial correlations of chains at the entanglements scale up to timescales of 300ns.
2. Nuclear magnetic resonance (NMR) data [31, 32, 33, 34] complement NSE, and also give information on orientation.
3. Dielectric spectroscopy is providing a complementary view of chain orientation dynamics to that of rheology, specifically measuring decay of end-to-end correlations of whole chains rather than averages over entanglement segments [35].

4. Small angle neutron scattering (SANS) of selectively deuterated material in quenched-flow experiments has started to reveal the nature of anisotropic structure on the length scale of the chain as a whole [36, 37, 38] under highly non-linear response.
5. Diffusion of polymers of varying architecture in different matrices is proving to be a sensitive test of co-operative relaxation of topology [39].
6. Dynamic light scattering as well as SANS on concentrated solutions has begun to test the consequences of theory for relaxation of composition fluctuations. This complements the information on chain orientation that tends to dominate the other molecular probes [40].
7. The efficacy of all these techniques is sharpened by the chemists' ability to synthesise monodisperse molecules of controlled architecture and deuterolabelling via anionic methods [37].

We will see in the following section that it has often been the combination of more than one experimental probe that indicates that our current theoretical models are problematical. The case of entangled star polymers (see below) is a case in point, for which rheological measurements in isolation give only green lights to a tube-dilation model, but when combined with dielectric spectroscopy indicate that the physics is actually more subtle.

The second qualitative new feature of the last ten years has been the rise of the power of simulation. It is now possible to conduct molecular dynamics simulations of, for example, elastically-connected Lennard-Jones polymers that contain 50 chains each of 10,000 monomers well into the regime in which entanglements dominate the dynamics [41], while a decade earlier the largest simulations feasible remained unentangled [42]. This technology is now at the point at which direct comparisons to experimental results such as NSE are now possible. The other advantage of large simulations is that they may mimic the “ideal” experiment in which everything may in principle be measured. This has been exploited in tests of fundamental theories of entanglements (see below) [43].

Thirdly, the growing quantity of data on branched molecules of controlled molecular weight and topology has provided severe tests of the tube concept at a level beyond that probed by linear chains [44]. The hierarchical nature of configurational relaxation at the molecular level in particular has been turned from speculation into orthodoxy. In the simplest case of entangled star polymers, the theory suggests that chains escape from their confining tubes not by reptation, which is suppressed by virtue of the immobile branch point, but by a process of *arm retraction*, present but largely eclipsed in the case of linear polymers (see figure 2). The effect on the viscosity of replacing linear molecules with those of identical molecular weight, but of star topology, is striking: now

$$\eta \sim e^{v(M_a / M_c)} \quad M_a > M_c \quad \dots\dots\dots(3)$$

is the dominant form of the molecular weight dependence, rather than $\eta \sim M^{3.4}$, where M_a is the molecular weight of the dangling *arm*.

Fourthly, as we have already hinted, the wealth of experimental and simulation data has sharpened the theoretical picture. Without exploding with new parameters, it has been possible to capture, in a single model, modes of entangled motion beyond pure reptation. In linear response *contour length fluctuation* (CLF), the Brownian fluctuation of the length of the entanglement path through the melt, modifies early-time relaxation. Similarly the process of *constraint release* (CR) we anticipated, by which the reptation of surrounding chains endows the tube constraints on a probe chain with finite lifetimes, contributes to the conformational relaxation of chains at longer times. Both the processes of CLF and CR contribute to the quantitative understanding of linear rheology, such that the $\eta \sim M^{3.4}$ law is no longer a mystery [45, 46], but much of the newer data still need to be examined quantitatively as sensitive tests of the detailed physics, and many puzzles remain. We will refer to these processes as we examine the potential of current experimental probes and theoretical treatments. For concreteness, they are visualised in figure 3. In strong deformations the additional processes of *chain stretch*, *chain retraction* and *branch-point withdrawal* emerge on the level of single chains (the latter exclusively in the branched case), and *convective constraint-release* (CCR) at the level of co-operative motion [47, 48, 49].

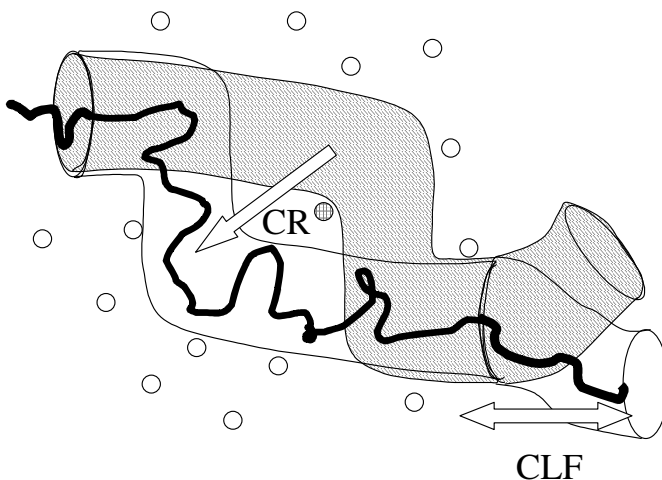


Figure 3: A cartoon of the processes of contour length fluctuation (CLF) and constraint release (CR) on a linear polymer in a constraining tube. In CLF the chain end retracts via longitudinal fluctuations of the entangled chain, but without requiring centre-of-mass (reptation) motion. Re-extension of the chain end may explore new topological constraints, reconfiguring the tube. In CR, an entanglement with a neighbouring chain (shown hatched) may disappear, allowing effective conformational relaxation of that part of the tube, again without reptation of the test chain itself. In both cases the former tube configuration is shown dark, the new, light.

Fifthly, a number of other theoretical frameworks have been proposed that do not invoke the tube concept directly [50, 51, 52]. Some of these are directly distinguishable in their predictions, others are not, but experimental groups producing new data have at times been in a quandary over which theory to compare to. Others begin with the tube idea, then make further approximations [53, 54]. Tools from dissipative hydrodynamics for discriminating at least between theoretical schemes that are thermodynamically permissible, and those that are not [55], has also been recently applied in the context of entangled polymeric fluids [56].

Sixthly, the fundamental work on entangled dynamics has progressed to such an extent that industry has begun to look intently at this programme of research to supply working tools in the development of new processes and products. Activities range from using theory-interpreted rheology to deduce molecular weight distributions [57, 58, 59], to the identification of long chain branching (LCB) by rheological means [60] and even early attempts at prediction of extensional rheology in processing from models of the polymer synthesis [61]. Numerical solutions to the equations of motion derived for polymer melts are becoming an attractive industrial research tool.

Finally, the field has grown sufficiently in confidence for the serious debate of a number of new physical processes until now omitted from tube models. Unsurprisingly, most of this conjectural ground lies in the domain of non-linear response. As always the choice is between modifying the model and building an entirely new framework from scratch, but the tube approach has proved in the past to be a paradigm within which many second-order effects can be accommodated. A recurrent example is the question of local deformation of the tube-diameter in a bulk strain [62, 63]. Detailed considerations of local stress balance within topological interactions may be related to this idea [64]. The consequences of dropping of the assumption of high flexibility of all subchains has been explored by Morse in a series of papers reconstructing tube models for stiff polymers [65, 66]. Residual effects of local stiffness may go some way to explaining recent detections of *non-universality* in the path-length fluctuations of entangled chains, or equivalently in the relation between the transitional quantities M_e and M_e that we have already defined [67, 68]. These departures from universal behaviour are either worrying or interesting, depending on one's point of view.

In the following sections, we will review in a little more detail some of the (arguably) most important current questions that the current state of research poses. Naturally they are related in ways that we as yet only partially understand - the present division may well seem arbitrary and contrived before long. Between them they cover ground from the fundamental to the applied, and from linear to highly non-linear physics. They are:

- What is the nature of the entanglement field?
- What is the nature of the anomalous terminal region of star polymers, where tube dilation breaks down?
- What is the general relation between local constraint release and tube dilation?
- What can ring polymers tell us about the melt state?

- What is the correct description of Convective Constraint Release in strong flows?

3. SOME CURRENT CHALLENGES

What is the nature of the entanglement field?

There has been a long history of attempts to derive the existence of the tube confining field from fundamental properties of Gaussian chains, rather than simply to work with it as an *ansatz*. There are three central questions facing such an approach:

1. Can we understand the emergent scale of the tube diameter?
2. What is the correct functional form of the dependence of tube diameter on polymer concentration?
3. How, if at all, is the tubelike constraint coupled to bulk deformations?

The difficulties facing a rigorous topological approach [69] is that entangled melts (rather than simple rings) do not possess true global topological invariants such as those that can be defined for closed knots and braids. Instead, locally defined topological states are the best that one can do [12, 70, 71]. In addition, only the simplest invariant of the “winding number” bears representation in terms of the familiar spatial arc coordinate representation of a polymeric fluid [72, 73]. This number is defined exactly for two loops, and quantifies the net number of turns that one loop makes around the other. If the two loops are electrically conducting, the winding number is also proportional to the mutual inductance of the loops. One can also show that forces can be transmitted via Brownian motion between chains that are only linked but not cross-linked [69]. Calculations that restrict the huge number of possible topological structures and invariants to the winding numbers can be made to produce results for the power-law with which an emergent confining field scales with polymer concentration. The density of links ρ_{link} varies quadratically with the density of loops, corresponding to a scaling of the entanglement-dominated plateau modulus with polymer volume fraction as $G \sim \phi_p^2$. This is close to experimental data, but there is significant evidence that $G \sim \phi_p^{1+\alpha}$ with $\alpha > 1$ [74]. The conceptual tool used in most approaches is the function $f_N(r)$, defined as the probability that two rings of N links, whose centres of mass are separated by a distance r , are linked. A good approximation to this function is [75]:

$$f_N(r) \cong 0.6 \exp\left(-0.3 \frac{r^3}{R_L^3}\right),$$

where R_L is the “linking radius”, close to R_g of the chains. The model of Graessley and Pearson, for example, [12] predicts that the elastic modulus of a rubber can be separated into a simple sum of a cross-link (“phantom”) contribution, and a linking contribution $a[f_N(r)]$ that is an integral functional of $f(r)$ and the chain density:

$$G = G_{phant} + b \cdot a[f_N(r)]\rho_{link}.$$

A recent simulation confirmed the effectiveness of the approximation that linking numbers are the dominant topological invariant for rubber elasticity [43] in the case of random networks, but found a strong under-prediction of the entanglement contribution to the modulus in specially-designed regular networks. This reference also gives a good summary of the field, including the opportunities now offered by computer simulation. But a fundamental problem faced by theories that depend on local winding numbers to explain the topological effects observed in rheology is that result that the winding number of two overlapping Gaussian random walks is controlled by the small-scale cut off to their Gaussian statistics. In flexible polymers this is of order of the monomer size, not the much larger tube diameter. This length scale itself is one suggestive piece of evidence that the key constraints are *non-local*, rather than local to a single interaction between two chains.

A second problem is that the winding number carries a sign - local topological interactions of two chains may have positive or negative twist. This means that the absolute value of the net total winding number of two interacting chains increases as the square root of the length of chain, not linearly as is represented by a tube model of entanglement. These issues may together be resolved by invoking *three*-chain interactions as the essential ingredient for entanglement. For the signed contributions of the windings between two chains may be frustrated from cancelling by the topological intervention of a third chain. Now the local degree of winding that may only be cancelled by diffusion of a free end scales linearly with the path length of chain. A single tube segment will have a size determined therefore by a critical number of such interactions, which will itself arise when a critical number of different chains pass through its volume

A further clue is provided by an important series of papers that point to the role of the “packing length”, p of a polymer in determining its modulus (or equivalently entanglement molecular weight. It was a considerable surprise when this recent very careful study of the rheological properties of many tens of different chemistries [67, 68] came to the conclusion that this sequence does *not* take place in a universal way, but that M_e , M_c and M_ρ all scale in a different way with the packing length of the polymer, p . This length, independent of the molecular weight of the chain, is defined as:

$$p = \frac{\Omega(N)}{R_g^2(N)},$$

where $\Omega(N)$ is the volume of melt occupied by the monomers of a chain of degree of polymerisation N . This may be determined simply from careful measurements of density, R_g is measured in the melt by neutron scattering. Both Ω and R_g^2 are proportional to N , so p is independent of molecular weight, and is usually between 2 and 10 Å. In a simple model of monomers in which they have a length l and a width w , $p = w^2/l$, the monomer width moderated by its aspect ratio. The observation that $M_e \sim p^3$ is consistent with the suggestion that an entanglement length (or tube diameter) is defined by a fixed number of other chains passing through the volume it spans [76]. It

also amounts to the statement that the tube diameter is universally an $O(10)$ multiple of the packing length of the polymer. But the other critical molecular weights scale in a different way: M_c is about twice M_e at low packing length, but falls proportionately as p rises. On the other hand, the molecular weight at which pure reptation is seen to dominate, M_p , falls from a high value of 10^3 at low packing length. The extrapolation at present is that all three molecular weights converge at $p \cong 10 \text{ \AA}$!

Although at first sight a shock, there is one grain of consistency with what we know about the underlying physics. The relative strength of CLF is responsible for the separate existence of both M_c and M_p from M_e , so if CLF is suppressed by increasing p , then this would indeed produce the observed effect. No more can be said at present without detailed rheological or dielectric experiments on monodisperse melts of high p , or without some inkling of the mechanism by which increasing packing length might suppress CLF in flexible chains.

Whatever the non-universalities that emerge, the non-local nature of entanglement is supported by a further current strand of work directed at the third question at the start of this section. To say anything about how the tube field deforms at large strains demands a plausible model for the field itself, and for how it couples into the bulk, affine deformation. An early application of the “replica method” of calculating partition functions in the presence of quenched disorder showed how calculations of both stress and single chain scattering functions could be made from specific models [77]. In that case the tube was modelled as a series of harmonically-localised constraints on monomers spaced by an entanglement along the test chain. Several groups have tackled this issue again recently in both real-space treatments [78], and by exploiting confinement of Rouse modes along test chains in a network [79, 80]. Both approaches sharpen our picture of the “tube”: for if the constraints on a test chain are modelled as elastic springs themselves, anchored to a set of points in the melt or network itself, then this set of constraint point is both highly non-local and highly disconnected. Put another way, a Gaussian chain is itself only marginally connected (it has no derivative), so if it is to be reconstructed by a convolution of a softening (harmonic) function taken over another set of points, then that set must be highly disconnected. In the eigenmode picture [79] where one writes a walk $\mathbf{R}(s) = \sum_p \mathbf{X}_p e^{ips}$, this feature emerges in the high wave-number amplitude of the harmonic coefficients \mathbf{X}_p of the “path” of anchor points - their mean square $\langle \mathbf{X}_p \mathbf{X}_{-p} \rangle$ is constant for the disconnected path of constraints, while it converges as $\langle \mathbf{X}_p \mathbf{X}_{-p} \rangle \sim p^{-2}$ for a connected Gaussian chain. If one assumes that the anchor points, delocalised from the chain itself, are far enough distributed within the network to deform affinely, then one finds that the tube diameter (defined by the root mean square fluctuations of monomers about their mean positions) *does* deform with the bulk, but sub-affinely, so that the α Cartesian component of the tube extends as $a_{\alpha} = \lambda_a^{1/2} a_0$ [78]. Evidence is beginning to accumulate that confinement due to entanglements differs from confinement due to crosslinks in that its strength does depend on the overall deformation of the system.

Clearly these fundamental considerations are at the point where they can begin to feed into the recent advanced models for strong deformation of entangled fluids.

What is the physics of terminal region of star polymers?

We recall that in branched entangled polymers, reptation is suppressed in favour of an activated retraction of the chain end in an effective potential $U(s)$, so that to a rough approximation the relaxation of a segment a path distance s from the free end as $\tau(s) \cong \tau_0 e^{U(s)}$. This fundamental idea [18, 81, 25] gave qualitatively the correct features of star polymer rheology, but required an artificial weakening of the entropic potential calculated from knowledge of the tube diameter if the relaxation times were not to be predicted exponentially too large. Clearly the effect of constraint release (CR) was essential to understanding the relaxation spectra of star, and other branched, polymers. The idea termed “tube dilation”, “dynamic dilution” or “dynamic tube dilation” (henceforth DTD) was introduced within tube models of entangled polymer melts first by Marrucci [82] in the context of linear polymers, then by Ball and McLeish for melts of star polymers [83]. It models the release of constraints on a test chain, as other chains reptate or retract away from its environment, as an effective widening of the tube (following a step strain for example). Although this approach to CR has not escaped criticism (see below), it has proved an extremely powerful and productive idea in the case of branched polymers. Indeed, although agreement of theories of CR based on tube dilation with experiments on monodisperse linear polymers is not good, agreement in the case of entangled branched melts and some linear blends is spectacular. Comparison of the DTD theory with experiments on stars [84], star-linear [85] and star-star blends [86], H-polymers [37] and combs [87] have all met with quantitative success. For a detailed review see [44].

The idea is motivated in the case of branched polymers by the observation that at the timescale when a segment a fractional distance x from the end of a dangling entangled arm is just being released by a deep retraction of the free end, all segments further out have been relaxed many times on exponentially faster timescales [83], so act as a diluent for the entanglement network. In this respect, the timescale separation is much better than for different segments along a linear polymer, so the theory might indeed be expected to apply to star arms. An approximation to Kramers' result for barrier hopping is used to evaluate the timescale for relaxation of a segment at $x + \Delta x$, assuming that all segments $x' < x$ act as diluent. If $U(x;n)$ is the (entropic) potential for retraction to a fractional distance x from the end of a tube containing an arm of n entanglements in a fixed network, and $\Phi(x)$ the function that evaluates the effective undiluted network fraction as a function of x , ($\Phi(x)$ depends on the presence of other slower segments in general), then the dynamic dilution *ansatz* becomes the “Ball-McLeish” (BM) equation [44]:

$$\frac{dU_{eff}(x)}{dx} = \frac{\partial U_0(x,n[\Phi(x)]^\alpha)}{\partial x} \dots\dots\dots(4)$$

where α is an exponent close to unity whose exact value depends on the yet-unresolved exact nature of entanglements [44] and $\ln\{\tau(x)\} = U_{eff}(x)$. The “dilution

exponent" α is related to the dilution of the plateau modulus G_N^0 with concentration of polymer ϕ_p such that $G_N^0 \sim \phi_p^{\alpha+1}$. So equation (4) allows the current primitive path length potential (on timescales at which tube segments at x are just released) to be diluted as if all relaxed chain segments were solvent. The "bare" potential for primitive path fluctuations $U_0(x, n)$ is one of the disputed ingredients of any theory of deep entangled retraction dynamics. The most common assumption, based on a model of a chain in a straight tube [88], is the quadratic form:

$$U_0(x, n) = \frac{1}{2} \nu n x^2 \quad \dots\dots\dots(5)$$

with $\nu = 3$ (we shall express all potentials in units of $k_B T$). But other values of the constant ν as well as non-quadratic corrections appear in lattice models [89]. In this section we shall retain a quadratic assumption for the bare potential, but keep the prefactor ν as a free parameter. In the case of a simple monodisperse star-like arms in a melt containing a fraction $1 - \phi_a$ of slower-relaxing material (such as comb polymer backbone [87] or very long linear polymer [90] and using $\alpha = 1$, the relaxation time equation becomes:

$$\frac{d \ln \langle \tau(x) \rangle}{dx} = \nu n x (1 - \phi_a x) \quad \dots\dots\dots(6)$$

So the DTD result for the effective potential that determines relaxation times of the segments along the dangling arms is

$$U_{eff}(x) = \frac{\nu n x^2}{2} \left(1 - \frac{2}{3} \phi_a x \right) \quad \dots\dots\dots(7)$$

The most striking agreement with experiment is met with in comparison with the ensemble of experiments representing changes in the effective value of star arm volume fraction ϕ_a . From pure stars ($\phi_a = 1$) to tracer stars in long linears ($\phi_a = 0$) via H-polymers and combs for intermediate values, exponential renormalisation of the star arm terminal time with concentration is consistent with expression (7) putting $x = 1$.

A specific criticism of this approach is that although it clearly renormalizes the potential in an plausible way, it does not appear to renormalise the effective diffusion constant for the barrier-hopping problem in a self-consistent manner. By choosing a larger tube in which to retract, the chain does indeed manage to reduce the differential height of the barrier it needs to overcome at each timescale to attain deeper retractions. However, it does this with the penalty of higher friction. The basic unit is not now a chain of monomers experiencing Rouse friction in a "bare" tube, but a chain of "blobs" themselves entangled on faster timescales, that only become effective free monomers when their appropriate tube scale is achieved by retraction, so conferring on them a much higher effective drag than the bare monomers. This exponentially-slower diffusion scale is not explicit in this treatment. Nor is it clear that the *best* choice for the retracting arm at any given stage of relaxation is to assume the *largest* possible tube diameter in which all relaxed segments act as solvents. A smaller choice is clearly

possible for retraction attempts, steepening the potential gradient but with the benefit of a larger effective diffusion constant.

A second, more general, criticism is to point out the absence of a demonstration that in the case of star-arm retraction, DTD is the correct limiting case of our more detailed current paradigm for treating CR in linear polymers. In this theory each release of a constraint by reptation of a neighbouring chain allows the tube of a test chain to “hop” a distance or order one tube diameter. Such a local stochastic dynamics endows the tube itself with Rouse-like dynamics. The local hopping rates of the Rouse tube are calculated self-consistently with the reptation times of the surrounding chains [74]. If the processes of reptation/fluctuation and Rouse tube motion are independent, the full relaxation function $G(t)$ may be written as a product:

$$G(t) = R(t)\mu(t) \dots\dots\dots(8)$$

of tube and chain relaxation functions. Using this approach, it is possible to show that DTD is correct for the terminal relaxation for *extreme bimodal blends of linear polymers only*. Describing the blend in terms of the number of entanglements of the long and short chains, n_L and n_S and concentration of long chains ϕ_L , we require $\eta_L > \eta_S^3$ and simultaneously that $\phi_L \gg \eta_L^{-1}$. These constraints correspond to the requirements that: (1) the renormalised reptation time of the renormalised, high-drag, long chains in the “supertubes” defined only by their mutual entanglements be *faster* than their “bare” reptation in the low-drag narrow tubes defined by all entanglements; (2) the long chains are indeed mutually entangled. This result [91] is suggestive of the reason that DTD appears to work for star polymers, as it points to the need for a wide separation of timescales between the bare relaxation of the test chain and the relaxation times of the entanglements defining the dilated tube. However, it falls a long way short of a proof. The difficulty lies, of course in the enormous range of timescales for CR events in the star melt arising from retraction dynamics. In the case of monodisperse linear chains, the majority of CR events all have a characteristic timescale of the reptation time.

Progress in meeting these two powerful criticisms has not, paradoxically, been assisted by the success of the DTD theory of branched polymers. Yet at last there are very recent experimental indications that all is not well. First, a careful recent assessment of experiments measuring both the self-diffusion constant and the viscoelastic terminal time of star polymer melts [92] has pointed out a discrepancy in the way that the product $D_{self}\eta$ scales with M_{arm} . This product is a sensitive test of theory because the factors depending exponentially on M_{arm}/M_e cancel, leaving only a power-law dependence. Strangely, although the magnitude of the product indicates a tube diameter for the diffusive hops of the stars as dilated, the *scaling* of the product is that predicted by assuming the hops take place in narrow, bare tubes!

Secondly, measurements of the dielectric relaxation function of well-entangled star polymer melts [93] have shown that although intermediate relaxations follow DTD predictions, the terminal behaviour is very different indeed. The dissipative part of the dielectric relaxation, $\epsilon''(\omega)$, shows a Maxwell-like *peak* at the terminal time, instead of the smooth continuous superposition of modes predicted by the DTD theory, and suggested by the rheological function $G''(\omega)$ (see figure 4).

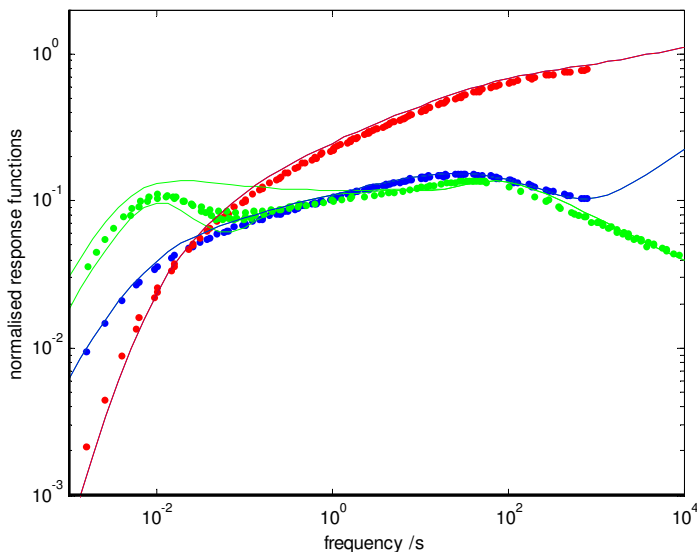


Figure 4: Dielectric and rheological data on a 6-arm PI star melt with $M_w/M_e = 16$ (by courtesy of H. Watanabe). Curves associated with the lower two functions (G' and G'') are predictions of the rheology by dynamic dilution [84], the upper (light) curve is its prediction for the upper data set for $\epsilon''(\omega)$. The peaked (light) curve is the prediction for $\epsilon''(\omega)$ of a theory in which dynamic dilution is arrested for the final 1/3 of the star arm, and all remaining response relaxed with the last entanglement.

Thirdly, a simulation that represents mutual entanglements in a star polymer melt as an ensemble of “slip-links” [96] connecting points on two star-arms in a numerical ensemble, has suggested that new physics does indeed determine the final relaxation of the innermost and longest-lived entanglements. Instead of a gradual widening of the tube (represented in the simulation by repeated replacement of “fast” entanglements in the vicinity of slow ones), the final relaxation is determined in this simulation by a diffusion of the very slowest and deepest entanglements along the arms towards the free ends, where they are met by retraction dynamics.

There is an urgent need to examine when and to what extent the DTD picture emerges from a more careful analysis of CR, along the Rouse tube picture employed in the case of linear polymers. Suggestions that this may now be possible, but only within a very much richer structure of activated dynamics, have recently been made [94]. We outline where this may lead in the following.

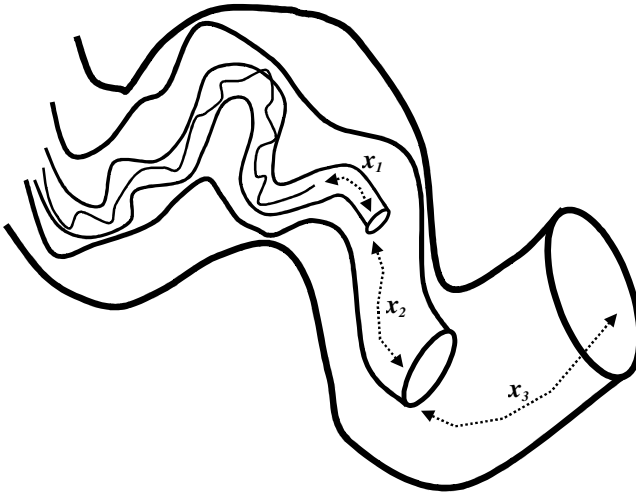


Figure 5: Conceptual diagram of a series of nested Rouse CR tubes in retraction dynamics, the larger tubes generated by slower CR events. The starlike-arm polymer chain is represented by the lightest line, slower Rouse tubes by increasingly heavier lines. Three retraction coordinates x_1 , x_2 and x_3 contribute to the total primitive path distance retracted.

In the case of the “supertube reptation” regime of DTD in bimodal blends of linear polymers, it was not essential to recognise that both ordinary chain-reptation in the bare tube, and renormalised reptation of the “bare” tube within the supertube *both* contribute to stress relaxation [91]. This is because in the case of stress-relaxation by reptation, the mean relaxation times are dominated by whichever process is the faster. However, in the case of *activated* diffusion that applies to entangled star arms, the simultaneous contribution of several modes can make a big difference. We already know that in a star melt, CR events have exponentially-separated timescales. Depending on the number of CR events at a given tube-scale required to constitute an effectively-independent super-tube that undergoes local Rouse motion, there may be several nested Rouse-like tubes contributing independently to the retraction dynamics of the star arm. In figure 5 we show how three independent levels of supertube may generate three coordinates that sum to give the total fraction of primitive path relaxed by a particular configuration.

Each mode represents an effective Rouse-like tube polymer, carrying the bare drag for the chain mode x_1 and renormalised drag for all tube modes x_i with $i > 1$. Furthermore, each of these effective Rouse polymer tubes carries the same overall topology of the branched starlike arm, so corresponds to a version of the original star arm in a quadratic potential for its own contribution to the primitive path length

retracted. Providing we know the number of independent modes x_i and their effective retraction potentials $U_i(x_i)$ and drag coefficients $\zeta_i \equiv k_B T/D_i$ we can restate the problem of the configurational relaxation of segments along an entangled starlike arm thus: a segment at primitive path coordinate x relaxes at the first passage time to the value x of the Brownian coordinate X defined by:

$$X = \sum_i x_i \tag{9}$$

with the initial condition $X = 0$. We may specify the relevant parameters $U_i(x_i)$ and ζ_i in a convenient way by assigning each mode a retraction co-ordinate \tilde{x}_i . We suppose that \tilde{x}_i is the maximal total retraction of neighboring chains required to set the tube diameter and effective drag of the supertube mode i . The potentials become:

$$U_i = \frac{\gamma Z x_i^2}{2} (1 - \tilde{x}_i) \equiv \frac{\beta_i}{2} x_i^2 \tag{10}$$

defining the set of quadratic potential strengths $\beta_i = \gamma Z (1 - \tilde{x}_i)$, and the effective diffusion constants (up to a prefactor of the dominant exponential dependence)

$$D_i(x) \equiv D_0 \frac{\tau_0}{\langle \tau(\tilde{x}(x)) \rangle} \equiv \frac{k_B T}{\zeta_i} \tag{11}$$

We note that, as in the last section, a more careful weighted sum over all CR events contributing to mode i is possible, but that since the slowest CR event of waiting time $\tau(\tilde{x}(x))$ is exponentially longer than the rest of the population, it will dominate the sum up to a prefactor. We have here also defined the parameters β_i and ζ_i that describe the effective quadratic potential strength and drag for each nested tube retraction mode x_i . Fortunately the solution to this problem for the mean first passage time is already known in the literature. The case for general potentials was stated in [95]. For the case of quadratic potentials the asymptotic result for $U(X) \gg 1$ can be cast in the form[#]:

$$\tau(x;t) = \frac{\sqrt{2\pi}}{x} \frac{\left(\sum_i \frac{g_i(t)}{\beta_i} \right)^{3/2}}{\left(\sum_i \frac{g_i(t)}{\zeta_i} \right)} \exp \left(\frac{x^2}{2 \sum_i \frac{g_i(t)}{\beta_i}} \right) \tag{12}$$

In the case of just a single mode this high-dimensional result reduces exactly to the asymptotic Kramers form as may easily be verified by setting the sums to their first terms only, β_i and ζ_i constant and $g_i = 1$ (see below). We have chosen to present first this intermediate form, parameterised by the time t itself, as it contains some important physics that will help us to determine which tube retraction modes to count in the calculation of the mean first passage time of any given tube coordinate x . Each time that the sum over contributing modes appears in (12), it is accompanied by an

[#] I am greatly indebted to Dr. A. E. Likhtman for pointing out both this reference and its consequence for summed quadratic degrees of freedom.

“ergodicity factor” $g_i(t) = (1 - e^{-2t/\tau_i})$ that approaches unity only at times of order of the relaxation time of the i^{th} mode $\tau_i = \zeta/\beta_i$ in its own quadratic potential. Alternatively this is the timescale on which that mode may explore the shape of its equilibrium distribution around the minimum of its potential - hence “ergodicity”. This is physically significant: clearly a very slow, high-drag supertube mode will not contribute to the retraction of a tube segment near the free end of the star-arm. So the ergodicity requirement shows that the expression for the first passage time (12) needs to be treated self-consistently: a mode cannot be included in the first passage time calculation of a coordinate x if its own ergodicity timescale τ_i is longer than $\tau(x)$. In a more exacting approach, one would put $t = \tau(x)$ in the terms $g_i(t)$ of (12) and iterate self-consistently.

The most remarkable feature of the structure of the solution (12) is the form of the modified effective potential when higher modes are present (the argument of the exponential in the expression). For it appears that we may add higher, slower, modes to the dynamics and reduce the effective barrier potential irrespective of the drag of these modes. In fact, as in our problem the higher modes are *softer* (have smaller β_i than the bare chain retraction mode with β_1), their addition to the dynamics very markedly reduces the effective barrier height. Even in the prefactor to the exponential containing the effective potential, the drag of the higher modes is not dominant. The controlling influence of their exponentially higher drag enters only *via* the ergodicity terms $g_i(t)$ that dictate whether or not they play in role in the retraction dynamics at a particular time scale t . We may understand this by the nature of activated processes: the typical approach to a high barrier (in each contributing mode) takes the timescale of the ergodic time of that mode – it is the *waiting* time for such an unlikely excursion that takes exponentially longer. So as soon as a supertube mode is “activated” after its ergodic time, it can explore retracted configurations on which the bare chain retractions can superpose. The effective drag is still dominated by the bare chain because this mode must always be present in series with the slower modes.

At the first approach, we may parameterise a “density of states” for tube retraction modes in a continuous way. If a new supertube mode arises whenever the effective tube diameter has increased by a factor w from its previous dilated value (we might expect physically realistic values for w to be of order 2 or 3) then the continuous density of states $\rho(\tilde{x})$ that captures this physics is:

$$\rho(\tilde{x}) = \delta(\tilde{x}) + \frac{1}{2 \ln w} \left(\frac{1}{1 - \tilde{x}} \right) \quad \dots\dots\dots(13)$$

The delta function generates the bare chain retraction mode, which is always present. The second term describes the nested tube modes. In terms of this density of states, the sum in the effective potential of (12) becomes (for modes that satisfy the ergodicity criterion):

$$U_{\text{eff}}(\tilde{x}) = \frac{1}{\beta_1} \left[1 + \frac{1}{2 \ln w} \left(\frac{\tilde{x}}{1 - \tilde{x}} \right) \right] \quad \dots\dots\dots(14)$$

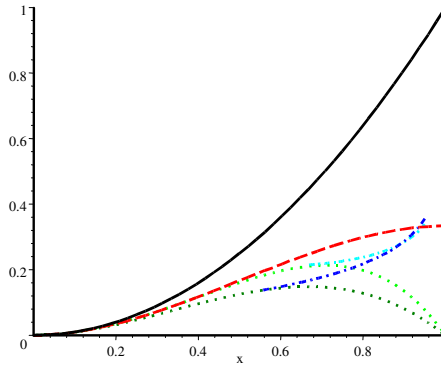


Figure 6: Results of the multimode supertube retraction theory for star arm first passage time. $\ln \tau(x)/(\gamma Z/2)$ is plotted against the retraction coordinate x (dotted lines) for two values of the density of states parameter $w^2 = e$ (lower dotted curve) and $w^2 = 6$ (upper dotted curve). The bifurcation in the curves indicates by the lower (unphysical) branch the result obtained if the ergodicity requirement is ignored. The upper (dot-dashed) branches indicate the physical solutions, after substituting for $\tilde{x}(x)$. We have set $\epsilon = 0.1$. The solid line is the normalised bare potential, and the dashed line the single mode result for full DTD ($U_{eff}(x)$).

where we have used $\beta_i = \beta_j(1 - \tilde{x})$. The application of this result in the first passage time is now just a question of the physical choice of the parameter w setting the overall density of states, and the form of the function $\tilde{x}(x)$. We recall that this was determined by an optimisation scheme in the one-dimensional theory. In this case, however, we have already determined (up to a parameter w) the distribution of modes and their effective drags. In this multimode theory the function $\tilde{x}(x)$ sets the limit of the slowest tube mode allowable in the current relaxation dynamics of x . In the limit of high molecular weight arms of Z entanglements, this ergodic criterion becomes asymptotic to full dynamic dilution so that $\tilde{x}(x) = x - 1/\gamma Z(\ln w)^2$ [94]. The final solution for the first mean retraction time problem up to prefactors of the exponential becomes:

$$\ln \tau(x) = \left(\frac{\gamma Z}{2}\right) \frac{x^2 \cdot 2 \ln w (1 - \tilde{x})}{2 \ln w + (1 - 2 \ln w) \tilde{x}} \quad \dots\dots\dots(15)$$

Plotting the results in the same form as a normalised effective potential in terms of dimensionless arc coordinate, we compare the results of this theory adopting

different density of states parameters w in figure 6, with those from a bare fixed tube, and from the simple dynamic dilution theory. Note that the form of the plot gives a normalised effective potential in the language of the former theory, removing the dependence of the height of the potential on both Z and the primitive path parameter γ . The two values chosen for the density of states parameter, $w^2 = e$ and $w^2 = 6$, give logarithmic relaxation times (or effective 1-d potentials) as shown dotted in the figure below the point of failure of the ergodicity criterion in maximal DTD, and dot-dashed beyond it. We might expect these two values to bracket the correct value on physical grounds - the first has the maximum density one could allow with sufficient independence between nested tubes, the second gives more room for independent motion of the tubes, but a rather sparse distribution that stretches the validity of the approximation of continuous mode distribution. Both choices of density of states give curves that initially follow the single mode full DTD result (dashed), then fall below it, before climbing once more towards it when the ergodicity criterion begins to affect the allowed values of dilated tubes *via* the non-trivial region of the function $\tilde{\chi}(x)$. This region is given by the upper branch of the bifurcated regions of the dotted curves - the lower branch indicates the unphysical non-monotonic result of ignoring the ergodicity criterion in both cases. The physically more reasonable choice $w^2 = 6$ (allowing 6 degrees of freedom per marginally entangled subchain in each supertube) follows the old DTD result rather more closely. So, although not an exact result, the DTD curve seems to approximate the results of simultaneously retracting nested supertubes, at least at the level of the exponential term in Z . There remains, of course, to calculate the consequences of pre-exponential factors and a more careful treatment of the ergodic introduction of the nested modes before any quantitative comparisons with data are warranted. However, the results at this level encourage further progress in these directions.

There are other consequences of this new picture of star-arm retraction. The failure of the ergodic requirement near $x = 2/3$ has a very noticeable effect on the dielectric spectrum, since this is controlled by the relaxation of the end-to-end vector of the remaining unrelaxed segments near the star-arm branch point [93]. No further dilation means that the dielectric relaxation of these segments is dominated by their longest renormalised Rouse time, *ie* the terminal time of the arm. This will be the mean relaxation time as observed by dielectric spectroscopy for *all* segments in a dipolar chain (of type A) from $x = 2/3$ to $x = 1$. To see how close this prediction comes to the new data, we have added to figure 4 a model calculation of $\epsilon''(w)$ in which the contribution from this final 1/3 of chain is reserved until the terminal time, keeping the full DTD result for the first 2/3. The result is rather close to the experimental results (arguably more persuasive that this is the right physics of the terminal peak than the suggestion of the rather minor “tube end effect” of reference [93]).

The breakdown of DTD at or around $x = 2/3$ predicted for pure stars is also related to the anomaly in the diffusion data. Indeed the nested tube picture suggests that, independent of the molecular weight of the star arm, the widest supertube mode accessible to it has a tube diameter $\sqrt{3}$ times larger than the bare “skinny” tube value. Without requiring lengthy calculations, we can see that the consequence of this for the scaling of the product $D_{self}\eta \sim Z^{-\sigma}$ is that the exponent σ should take the same value

as the prediction of [92] for diffusive hopping in bare tubes, but that the mean square hop distance (communicated to the value of D_{self}) should be about 3 times larger than the absolute value predicted by the bare tube theory. This prediction is in very close accord with the experimental results [92]. Calculations for relaxation of star-like arms in the presence of slower material also give results in close accord with experiment [94].

The density of states parameter should, in principle, be determined with no freedom. One possible approach is to insist that when all the nested tubes are accounted for, there should result the same density of degrees of freedom as the melt of phantom Rouse chains without entanglement. A calculation on these lines [94] gives $w^2 \cong 4.5$, which is indeed between the two values we chose to bracket the range of calculations in our case studies. A more nuanced calculation is certainly possible, but should be combined with the other improvements we have already identified.

This nested tube approach is also related to a recent sliplink simulation that accounted in part for some of the new dielectric data [96]. The simulation appears to be equivalent to a *two*-dimensional version (slip-link diffusion and chain retraction) of the current theory. This is expected to be very close to the results given by our continuous mode distribution for values of w^2 as large as 6, because most of the relaxation spectrum is then dominated by the operation of one or two modes only.

Perhaps the clearest summary of this work is that it begins to remind us of the fearsome complexity of the problems of entangled polymer dynamics that we have become accustomed to finding tamer than we strictly should. The power of simple ideas such as the tube itself, and of additional ideas such as tube dilation, can sometimes mislead us into oversimplifications of the very complex and high-dimensional problem of the full dynamics. In particular, we should anticipate that a full account of star polymer retraction, respecting high degrees of freedom should also take account of the contribution of all the *internal* Rouse modes of the original chain and Rouse-like supertubes. The full mode sum will therefore need to be over two indices rather than the single supertube index to which we have restricted ourselves in this work. There are indeed experimental indications from the subtle system of stars with one asymmetric short arm that indicate that modifications to the theory at least at this level will be necessary [97].

4. WHAT CAN RING POLYMERS TELL US ABOUT THE MELT STATE?

We know that many characteristics of the crystalline, glassy and fluid states of polymers rely on the special properties generated by the ends of the molecules – so what if there were none? What would be the nature of macromolecular matter composed entirely of loops? In particular, the tube theory of rheological response seems at first glance to revolve around the presence of ends. Whether by reptation, contour length fluctuation, or retraction, it is the passage of free ends through the entanglement field that generates stress relaxation and flow. Recent advances in the understanding of concentrated solutions and melts of unentangled rings continue to indicate that these systems possess particular fascination. They promise to furnish yet another class of entangled fluid, as qualitatively different from linear and branched systems as they are from each other.

Experimental investigations of concentrated rings are not new. In 1985 Jacques Roovers turned the technique of anionic polymerisation to make small quantities of monodisperse polystyrene rings [98]. The motivation then was the growing interest in the dynamics of polymer melts, when topological entanglements between chains dominate. Linear, star-shaped and H-shaped molecules had demonstrated that the architecture of the molecules at this global level dominated the viscosity and viscoelasticity of the melt more powerfully than their chemistry or molecular weight. As we have seen, the timescales for stress-relaxation in flow can be exponentially long as a function of molecular weight if the molecules carry a branched topology. At the same time, the tube model was beginning to find explanations for these effects. The key step is to find how long a locally-trapped region of the melt needs to wait for a chain end to diffuse by and liberate it. But if there were no ends to be found?

Answering this question turns out to be delicate. Roovers found (correctly) that the relaxation times of the ring-melts were much less than linear melts of the same molecular weight, but other groups initially disagreed, finding that the relaxation times were comparable [99]. However, the synthetic chemistry involved turned out to be much more delicate than in the case of monodisperse linear polymers. It is essential to synthesise rings that are not interlinked – although such “olympic gels” are themselves interesting as rubbery solids with no molecular cross-links at all! Moreover it became clear that any linear polymer contaminant in a melt of rings alters the dynamics out of all proportion to their concentration – bringing relaxation times rapidly up to linear melt values [100]. An additional challenge to interpretation was the familiar one that the initial material worked with, polystyrene, suffers the drawback of its high value of M_e (arising from the bulky side groups) that diminish the effects of entanglement.

None of this prevented a parallel theoretical development, however. Although linear chains in dense melts take on the statistical properties of ideal random walks, this now commonplace result was predicted *not* to hold for a melt of rings [101]. The topological constraints that they are not linked, frozen into the system from its inception, biases their conformations sufficiently so that, not just in magnitude, but even the way that their size scales with molecular weight should be weaker than for linear chains. As for dynamics, rather than the snakelike “reptation” of linear chains along their tubelike path of constraints, out best guess at rings seems to resemble more the amoeba – unentangled loops continually thrust out and retracted in the complex hedge of constraints imposed by neighbouring molecules [102] (see figure 7). This rearrangement of loops occurs on all length scales, and is responsible for a unique scaling of terminal relaxation time with degree of polymerisation in a fixed network of obstacles:

$$\tau \sim N^{5/2}. \quad \dots\dots\dots(16)$$

The diffusion constant, by contrast, is predicted to scale in the same way as in linear melts, with $D \sim N^{-2}$.

Without ready supplies of material to test these intriguing ideas, the natural recourse has been simulation. Some very recent work [103] provides strong hints that the earlier theoretical ideas may have been on the right track, especially for the terminal time. Simulated rings are indeed more compact in the melt, and relax considerably faster than their linear homologues. However, the simulated diffusion

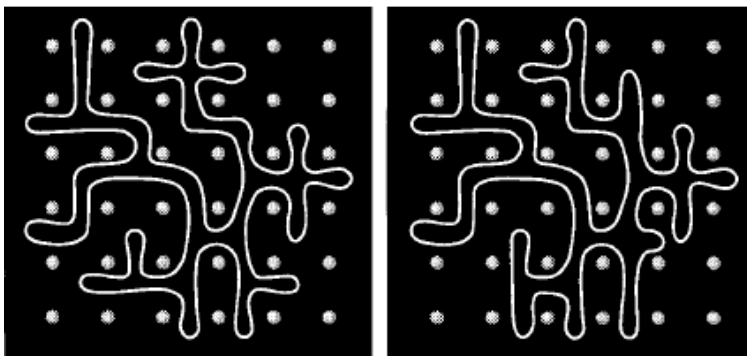


Figure 7: Basic dynamical moves of an entangled ring polymer, from [102]. The obstacles represent the constraints of other rings. A molecule reconfigures by rearranging its constituent loops on all length scales.

data suggest $D \sim N^{-1.6}$. This is not a fundamental issue of principle, however, since the theoretical picture for a true *melt* of rings is still very unclear indeed. In addition to the loop reconfiguration by retraction and re-entanglement, in the melt constraint release is also operative. Even less clear is how this will alter the stress relaxation function itself. The loop mechanism re-introduces dynamical scaling into an entangled system (the scaling property $G(\omega) \sim \omega^z$ (with $z = 0.5$) of the relaxation dynamics of Rouse linear chains is lost by entanglements), but whether there is a unique scaling, or a cross-over from loop-dominated to CR-dominated regimes is presently unclear from either simulation or experiment.

A new catalytic route to the manufacture of unlined rings [104] may provide a very welcome opportunity answer to these long-begged questions. The advantages of the new synthetic route are many: the rings are very unlikely to be linked, linear contamination is small, and the chemistry applies to the well-entangled polyolefin family. There seems no reason why pre-deuterated monomer should not be used so that the materials may be subjected to small angle neutron scattering (SANS), so allowing direct measurements on confirmation and dynamics at the molecular level. Large quantities are even attainable. A minor drawback is that the spread of molecular weights is not as narrow as that in principle obtainable from anionic methods, but exponentially distributed so that $M_w/M_n = 2$. Nevertheless, rheological, diffusion and scattering experiments on a range of molecular weights of these new materials must be an early priority to check the scaling-law predictions of the “amoeba dynamics” theories. They should also generate the impetus to turn the theoretical tools developed for linear and branched melt to the case of rings.

5. WHAT IS THE CORRECT DESCRIPTION OF CONVECTIVE CONSTRAINT RELEASE?

We have seen that two related anomalies of the tube model have remained stubbornly resistant to efforts to include even the subtle aspects of chain stretch and chain connectivity in strong flows: the phenomenon of shear thinning is greatly overpredicted, resulting in a non-monotonic variation of shear stress with shear rate, and the anisotropy of the single chain structure factor in shear is predicted to increase up to a factor of $Z^{1/2}$. The maximum in the flow curve is not seen in experiments on well-characterised polymer melts and entangled solutions [105] (although it does seem to be present in entangled wormlike surfactant solutions [106]). Nor is the high chain anisotropy seen in SANS experiments in shear [36]. The problem clearly arises from the spurious perfect alignment of the tubes along the flow-direction predicted by any model that allows only affine convection of tube segments. In an attempt to relax this simplification in a physical but simple way, Marrucci [47, 107] proposed a new type of constraint release arising from the convection of surrounding chains by the flow, which he called Convective Constraint Release (CCR). We have seen that in linear response, the arrival of a neighbouring chain end at a confining tube for a test chain allows a local reconfigurational relaxation of that chain segment (see figure 3). Without flow, the CR-generating events were caused by reptation or CLF of the neighbouring chains as aspects of their Brownian motion (these processes have been termed “thermal CR” [35]). However, we have seen that in strong flow a forced, non-stochastic motion of chain ends enters *via* the process of chain retraction. Now, at least when the chain stretch is only marginally perturbed from equilibrium, and possibly beyond into the stretching regime, the rate of tube-loss from retraction grows proportionally with the bulk deformation rate, so is a candidate for finite configurational relaxation towards equilibrium. Moreover, since the rate of the CCR relaxation process follows the bulk deformation rate, continuous relaxation of the tube contour is achieved however fast the flow! Such “Convective Constraint Release” (CCR) becomes increasingly important with shear rate and at some point should dominate the chain motion.

Marrucci [47] suggested that CCR be taken into account by correcting the reptation time by a term proportional to the chain retraction rate:

$$\frac{1}{\tau} = \frac{1}{\tau_d} + \beta \mathbf{K}(t) : \langle \mathbf{u}(t) \mathbf{u}(t) \rangle, \quad \dots\dots\dots(17)$$

where \mathbf{u} is the tangent vector of the primitive path, $\mathbf{K}(t)$ is the shear rate and τ_d is the reptation time (we recognise the double-contraction as proportional to the relative velocity of chain and tube). The $O(1)$ number β is necessary for the same reason as the equivalent constant c_v we introduced in linear response CR: the number of CR events required for each local tube reorientation is unknown.

Mead, Larson and Doi [48] developed this approach to CCR in a similar way in a set of constitutive equations for the tube orientation tensor and chain stretching. When $\dot{\gamma}\tau_R$ is large and both chain-stretch and CCR are operating, it is necessary at this level to redistribute the effect of CCR from orientational relaxation at low $\dot{\gamma}$ (*via* renormalising the effective reptation time as in [17]) to relaxing the *stretch* at high $\dot{\gamma}$.

They employed a “switching” function that deploys the effect of CCR from orientation and stretch relaxation with increasing flow rate. A much more sophisticated version in which path length coordinates are retained allowed adoption of CLF at the same level as equation (17) [48]. These approaches predict a final plateau of the steady state shear stress as a function of shear rate, and can achieve a good fit with data on $\sigma_{xy}(\dot{\gamma})$ and $N_1(\dot{\gamma})$ over a range of shear rates, but the plateau is approached from *above* for any reasonable value of the parameters β *i.e.* the stress maximum is *still* present! The version without stretch requires $\beta \cong 3$ to avoid the maximum, but this is hard to reconcile with the much smaller values required in linear response. A further drawback of these approaches is that information on the structure of the entangled chains is lost by allowing CCR to affect only the global stress relaxation time. This still leaves unexplained an important data set on the single chain structure factor in a sheared melt probed by small angle neutron scattering (SANS) [36]. A recent assessment of the MLD theory using entangled monodisperse and binary-blend PS solutions confirmed that the introduction of CCR was essential to capture the steady-state values and rates at which overshoots appeared, but found the magnitude of the overshoots in $\sigma_{xy}(\dot{\gamma})$ and $N_1(\dot{\gamma})$ to be consistently under-predicted. Non-spatial stochastic simulations have also introduced CCR *locally* on chains in the same way as in [108], yet also predicted a weak stress maximum. This seems to be because the way CCR is introduced in all these cases serves to reduce the stress from the Doi-Edwards result. Real chains seem to find a way to *increase* it. Yet it is clear that CCR is of overwhelming importance and dominates the dynamics and configuration of entangled linear chains at high flow rates.

A recent, more detailed approach to this problem (for non-stretching chains) treats CCR at a nearly equivalent level to CR (making the approximation of a single frequency of CR events, rather than respecting the distribution), by keeping the coarse grained coordinates of the chain, and allowing CCR events to generate local Rouse jumps of the tube [49, 109]. The idea is to retain full information about average chain trajectories instead of working indirectly with dynamic equations for the stress and orientation tensor. This approach also allows quantitative predictions about the single chain scattering function $S(\mathbf{q})$, and to develop a *local* description of CCR events. The main assumptions of the first version of the theory (valid when there is no chain stretch) are: (i) that CCR operates locally in reorienting chain segments both into and away from the flow direction, and (ii) that neither the number of entanglements per chain $Z = M/M_e$ nor the tube diameter a changes. The first assumption endows the tube itself with a Rouse-like motion in which the local hopping rate is coupled to the global deformation rate via a single new parameter. The second (constant length) assumption introduces a difference from ordinary Rouse-chain motion, and limits the range of validity at first (but see below) to $0 < \dot{\gamma} < 1/(\tau_e Z^2)$.

No single set of variables will be able to diagonalise the essential entangled modes of motion, namely (i) chain reptation, (ii) chain retraction, (iii) tube-length fluctuation and the new mode (iv) Rouse-tube motion. However, the theory is conventionally cast in a real-space notation for the tube trajectory $\mathbf{R}(s,t)$ and its tangent curve $\mathbf{R}' \equiv \frac{\partial \mathbf{R}}{\partial s}$, functions of curvilinear distance s from along the tube and

time t . Our chains are monodisperse containing Z entanglements of tube diameter a . The (stochastic) equation of motion becomes:

$$\mathbf{R}(s, t + \Delta t) = \kappa \mathbf{R} \Delta t + \mathbf{R}(s + \Delta \xi(t), t) + \Delta t \left(\frac{3\nu}{2} \frac{\partial^2 \mathbf{R}}{\partial s^2} + \mathbf{g}(s, t) \right) + \Delta t \lambda \left(\frac{Z}{2} - s \right) \frac{\partial \mathbf{R}}{\partial s}. \quad \dots\dots\dots(18)$$

The first term describes affine convection of the tube segments. The second is the well-known reptation form in which the noise term has a variance related to the curvilinear diffusion constant D , $\langle \Delta \xi(t) \Delta \xi(t') \rangle = 2D \delta(t - t')$. The third term describes the new Rouse motion of the tube. It has exactly the same form of deterministic and stochastic noise terms as the usual Rouse equation for chains, and they are coupled by the same fluctuation-dissipation relation. However the rate ν is not controlled by temperature, but by the rate of CR from other chains. Counting the entanglement release rate of all chains from retraction and reptation gives a self-consistent relation

$$\nu = c_\nu \left(\lambda + \frac{12}{\pi^2 Z^3 \tau_e} \right) \text{ where } \lambda \text{ is the retraction rate of the chain, set by the constant-}$$

length condition $\int_0^{\eta} |\mathbf{R}'| ds = Za$. The number c_ν is, as in linear-response CR and early versions of CCR the one new parameter in such a theory - $c_\nu = 1$ would correspond to one constraint release event giving rise to one local hop of an entanglement segment. We might therefore expect a rather smaller value than this, given the $O(10)$ number of chains involved in an entanglement [67]. The fourth term accounts for the retraction of the chain within the tube in a pre-averaged approximation in which the relative velocity of chain and tube increases linearly from the chain centre at $s = Z/2$. The retraction rate λ appears again as a prefactor. It is also possible to add a fifth term as a representation of [49]. Stochastic breathing-mode retractions of the chain end replace the tangent vector at s with a stochastic vector \mathbf{u} chosen randomly from the unit sphere (with a careful choice of the correlation $\langle \mathbf{u}(s) \mathbf{R}'(s') \rangle$). The rate of this process $1/\tau(s)$ is the same as that calculated for the local stress relaxation of entangled star-polymer arms [45]. Its inclusion allows the non-linear theory to reduce to a quantitative theory for the chain dynamics in linear response.

The real-space Langevin representation (18) is convenient for describing the physics, but not for performing calculations. More useful is the matrix second moments of the chain tangent vectors $\mathbf{R}'(s, t)$ defined by:

$$f(s, s', t) = \left\langle \frac{\partial R_\alpha}{\partial s}(s, t) \frac{\partial R_\beta}{\partial s}(s', t) \right\rangle - (\delta_{pq})_{\alpha\beta}. \quad \dots\dots\dots(19)$$

A decoupling approximation is applied to averages of λ and \mathbf{R} to derive an equation of motion for $f(s, s', t)$.

Setting $c_\nu = 0$ in this scheme generates a non monotonic shear stress response in steady flow, closely following the standard Doi-Edwards prediction, but adding a small amount of local CCR such that $c_\nu > 0.06$ removes the shear stress maximum

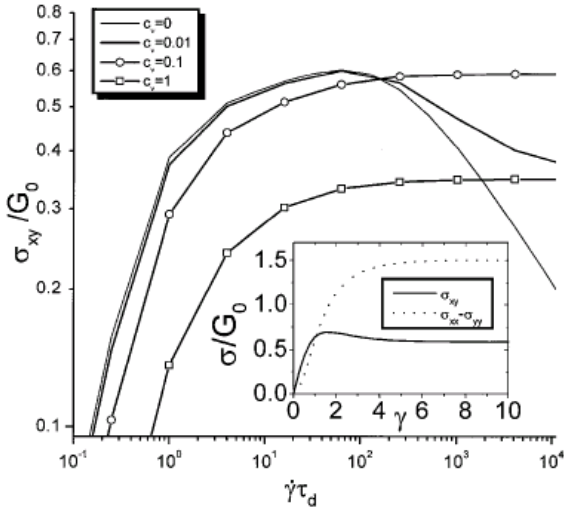


Figure 8: Predictions of the local-CCR theory for the steady-state values of shear stress with shear rate for various values of the CCR parameter c_v . The inset displays the predicted shear stress and normal stress transients in the limit of high shear rate (but with no stretch) for $c_v = 0$ (from [49]).

entirely; instead the shear stress tends monotonically to a plateau at high shear rates (see figure 8 for results in the large Z - for smaller Z the response is very nearly the same, with shifts to G_0 and τ_d from rapid end-fluctuations).

Increasing the rate of local CCR continues to enhance the shear stress at high shear rates, while decreasing it at low rates. The transient approach to the steady state exhibits a maximum for $\dot{\gamma}\tau_d > 1$, as observed in experiment. The opposite behaviour at low and high shear rates can be understood from the way CCR operates: at low rates the tube configurations are nearly isotropic so the additional relaxation mechanism simply speeds up the return to equilibrium, reducing the stress. However at high rates the tubes are nearly aligned in the flow direction in the absence of CCR; introducing it generates random buckles in the tube contour that protrude distances of order a in the flow gradient direction. Subsequent deformation of these buckles generates in turn immediate contribution to shear stress, which is therefore larger than without CCR. Omitting this symmetry can lead to problems: It is tempting, but incorrect, to permit CR events to smooth local tube contour but not to roughen it [108]. In fact at shear rates $\dot{\gamma} \sim \tau_d^{-1}$ there is only weak perturbation to the melt structure on the length scale of an entanglement strand so there is no reason to suppress the natural symmetry of tube-Rouse motion incorporated in [18]. Moreover the level of coupling of chain

retraction to CCR indicated by values of $c_v \cong 0.1$ corresponds to $O(10)$ retracting chains per tube-Rouse hop. This compares favorably with the universal number of chains involved in a single entanglement [67].

A typical structure factor computed from our theory is shown in figure 9. Constraint-release drastically changes the overall picture from tube theory without CCR: the degree of orientation decreases, and the q -dependence of the orientation angle appears; contour lines of $S(q)$ at smaller q are more oriented in the flow-gradient direction than at larger q .

To compare these results with neutron scattering experiments, we can extract various quantities including the characteristic dimensions $R_{max}^2(\dot{\gamma})$ and $R_{min}^2(\dot{\gamma})$ in the major and minor principal directions, as well as the q -dependent alignment angle $\beta(q, \dot{\gamma})$ between the major principal axis contours of $S(q)$ and the flow (x) direction. These quantities summarize the changes in dimension and orientation of typical chain conformations as a result of the flow, assuming that the contours of $S(q)$ are elliptical. The dependencies of β on both q and $\dot{\gamma}$ are shown in the inserts to figure 9, and are in qualitative agreement with existing experiments [36]. In particular both experiment

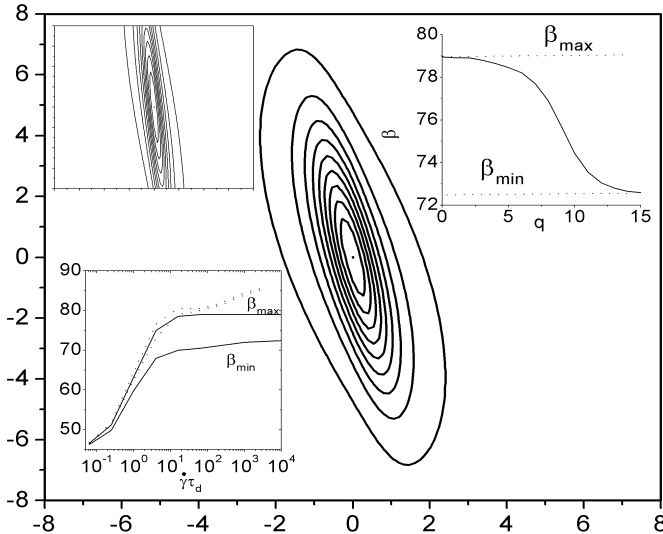


Figure 3: Steady-state scattering patterns calculated from a theory allowing CCR and original Doi-Edwards (insert top left). The axes of q_x and q_y are in units of the inverse tube diameter a^{-1} . Other inserts indicate behaviour of the angle of the principal axis with shear rate and q .

and this theory agree that the mean square radius of gyration in the flow direction never grows by more than a factor of three, and local CCR is able simultaneously to account for the chain anisotropy and the rotation of the principal axis of the scattering pattern with q . The latter is a striking feature of the data, and is a direct consequence of the local Rouse “buckling” of the tube, and the convection of the perturbed structures so formed to longer length scales by the flow. This is just the same process that led to the erasure of the shear stress maximum discussed above.

Local CCR calculations can be modified for the case of living polymeric micelles [109]. In this case local CCR is much less effective in removing the stress maximum than in the case of polymer melts; the maximum persists until a value of $c_v \cong 0.3$. So in the physically reasonable range $0.06 < c_v < 0.1 < 0.3$ this theory is able to account for the simultaneous absence of a stress maximum in melts and its presence in living micelles.

The addition of chain stretching is a natural next stage to the theoretical development of a contour-variable account of CCR, just as in the single-mode approximations of [47] and [48]. This can be done at the level of the Langevin equation for the contour coordinates $\mathbf{R}(n,t)$, equation (18), by adding a term that accounts for the curvilinear motion of monomer driven by local gradients in chain tension (itself proportional to the local stretch $\mathbf{R}'(n,t)$). This now replaces the term previously keeping the tube length constant in equation (18). The stochastic equation in $\mathbf{R}(n,t)$, (18), acquires a new term that reads:

$$\mathbf{R}(n,t + \Delta t) = \dots + 3D_c Z \frac{(\mathbf{R}' \cdot \mathbf{R}')}{|\mathbf{R}'|^2} \mathbf{R}' + \dots$$

and is supplemented by an expression for the CCR rate $\nu = c_v \lambda$, where the retraction rate is counted from the rate of tube loss at the chain ends [110]. Calculation proceeds in the same way as in the non-stretching case by passing to the Fourier representation of the tensor correlation functions of $\mathbf{R}(n,t)$. This more complete model predicts a near-plateau of $\sigma_{xy}(\dot{\gamma})$ between $\dot{\gamma}\tau_d$ and $\dot{\gamma}\tau_R$, and an increase proportional to $\dot{\gamma}^{1/2}$

beyond that (so that the “shear-dependent viscosity” $\eta(\dot{\gamma}) \sim \dot{\gamma}^{-1/2}$ (see figure 10). As with the non-stretching case, decoupling approximations are required to derive closed equations for the necessary correlation functions $\langle \mathbf{R}(n,t)\mathbf{R}(m,t) \rangle$. The quality of these approximations can be checked by simulation, but also by thermodynamic consistency. One issue concerning the possibility of new physics should, however, be raised in theories of CCR that are both local and non-linear. In fast flows, the primitive path length of the chain can be far greater than at equilibrium. This introduces (at least) two choices into a theory at this level for the *density* of CR events along the chain. We might assume either that the number of constraints along the chain were constant independent of stretch (so that the long CR Rouse relaxation time is independent of the flow rate and stretch). Alternatively, we might suppose that constraints of this dynamic kind are met with at constant contour density along the principal path. In this latter case, the CR Rouse relaxation rate is actually increased quadratically with chain stretch. Of course this choice touches deeply on the local physics by which the entanglement field arises. At the same level of importance now

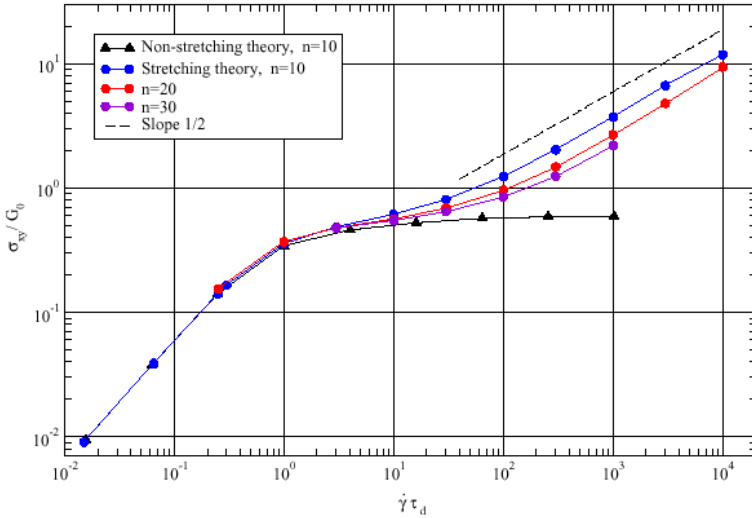


Figure 10: Predictions of the local CCR model with chain stretch using $c_v = 0.1$ for values of $Z = 10, 20, 30$. A comparison to the non-stretching version is given.

enters the assumption about the tube deformation itself in such strong flows [110, 111]. Initial investigations at this level suggest that the *transient* shear and normal stress overshoots are very sensitive to the choices made. A detailed comparison of this model (and its variants) with data from both transient rheology data as well as SANS chain structure factors will guide the next developments of theory. Excellent data sets in transient response in shear [112, 113], and more recently extensional response exist for entangled solutions. However, these are naturally limited in the degree in entanglement obtained (polymer concentrations are typically less than 10% to avoid elastic instabilities). Future strong flow data on monodisperse melts will be very important.

We should note a recently-discovered connection between the local CCR theory and the Marrucci and MLD versions without explicit chain coordinates. If only the lowest Fourier mode (tube Rouse eigenfunction) in the full theory is retained then a constitutive equation equivalent to the use of equation (17) results:

$$\dot{\boldsymbol{\sigma}} = \mathbf{K} \cdot \boldsymbol{\sigma} + \boldsymbol{\sigma} \cdot \mathbf{K}^T - \frac{2}{\tau_d} (\boldsymbol{\sigma} - \mathbf{I}) - \frac{2}{3} \text{tr}(\mathbf{K} \cdot \boldsymbol{\sigma}) \{ \boldsymbol{\sigma} - \beta (\boldsymbol{\sigma} - \mathbf{I}) \},$$

but with an *expression* for β in terms of the physical parameters of the full model ($\beta = 3\pi^2 c_v$). The large prefactor of $3\pi^2$ in this ostensible $O(1)$ number perhaps indicates

why such a large value is needed to overcome the shear stress maximum in that model. The stretching case gives an interesting “single mode” equation (the ROLIEPOLY equation - for ROuse LInear Entangled POLYmer) under similar treatment, but which indicates again the utility of molecular thinking even in the derivation of “toy” models for phenomenological application.

We have come a long way from the early reptation-only approximations, keeping also the subtler entanglement modes of CLF, CR, CCR, chain stretch and retraction in the model able to describe not only bulk properties but also mean chain configurations at the tube scale a and above. However, there are still physical effects that may be just as important not accounted for, and there has yet to be a proper assessment of the self-averaging approximations of all theories that work with the dynamics of a mean chain, rather than taking the average after solving the dynamics of a many-chain ensemble.

6. CONCLUSIONS

Although the field of molecular polymer rheology is a relatively mature one, there are clear signs that it is entering another extremely productive phase. There is no single source driving the current creativity, but we have pointed to a range of new experimental techniques working at the molecular level, several new theoretical ideas, and improved synthesis of model and industrial materials that together are defining the new challenges. It remains an especially satisfying area to work in because of the wide range of disciplines that are involved. We have not stressed in the above, though might have done, the example of “multiscale modelling” that is furnished by molecular rheology. As better constitutive equations, properly reflecting entanglement-level structures, appear, they immediately allow consequences of engineering at the molecular level to be computed in macroscopic flows (see the article by R. Keunings in this volume). There is every reason to hope that future consequences will include a deeper understanding of topological interactions underpinning entangled dynamics on the one hand, and tools that industry might actually use in the design of processes and products, on the other.

ACKNOWLEDGEMENT

I have benefitted hugely from discussions with many colleagues in the preparation of this article and its background, but in particular would like to thank Sam Edwards, Masao Doi, Ron Larson, Scott Milner, Michael Rubinstein, Ralph Colby, Ralph Everaers, Robin Ball, Mike Cates, Lew Fetters, Oliver Harlen, Kevin O'Connor, Nigel Clarke, Graeme Bishko, David Bick, Daniel Read, Richard Blackwell, Sasha Semenov, Alexei Likhtman, Tam Sridhar and Hiroshi Watanabe. Thanks are due to the Kavli Institute of Theoretical Physics, UCSB, for hosting a workshop in April 2002 that formed the genesis of this article.

REFERENCES

1. Flory P J, “Principles of Polymer Chemistry”, Cornell University Press, Ithaca, (New York) (1953).
2. Zimm B H and Stockmayer W H, *J.Chem. Phys.*, 17 (1949) 1301.
3. Edwards S F, “The configuration and dynamics of polymer chains”, in “Molecular Fluids”, (Editors: Ballab R and Weill G), Gordon and Breach, (London), (1976) 151-208
4. Kuhn W, *Kolloid Z.*, 68 (1934) 2.
5. Zimm B H, *J. Chem. Phys.*, 24 (1956) 269.
6. Rouse P E, *J.Chem. Phys.*, 21 (1953) 1272.
7. Zinn-Justin J, “Field Theory and Critical Phenomena”, Clarendon Press (Oxford) (1993).
8. Ferry J D, “Viscoelastic Properties of Polymers”, Wiley (1986).
9. Adam M and Delsanti M, *M. J. Phys. France*, 45 (1984) 1513.
10. Treloar L R G, “The Physics of Rubber Elasticity”, Clarendon Press (Oxford), (1975).
11. Ball R C, Doi M, Edwards S F and Warner M, *Polymer*, 22 (1981) 1010.
12. Graessley W W and Pearson D S, *J. Chem. Phys.*, 66 (1977) 3363.
13. Small P A, *Adv. Polym. Sci.*, 18 (1975) 1.
14. Meissner J, *Pure Appl Chem.*, 42 (1975) 551.
15. Hansen D R, Williams M.C. and Shen M, *Macromolecules*, 9 (1976) 345.
16. Edwards S F, *Proc. Roy. Soc. London*, 92 (1967) 9.
17. de Gennes P G, *J. Chem. Phys.*, 55 (1971) 572.
18. de Gennes P G, *J. Phys. (Paris)*, 36 (1975) 1199.
19. Doi M and Edwards S F, *J. Chem. Soc. Faraday Trans 2*, 74 (1978) 1789; Doi M and Edwards S F, *J. Chem. Soc. Faraday Trans 2*, 74 (1978) 1802; Doi M and Edwards S F, *J. Chem. Soc. Faraday Trans 2*, 74 (1978) 1818; Doi M and Edwards S F, *J. Chem. Soc. Faraday Trans 2*, 75 (1979) 38.
20. For a lighthearted and alternative view of this story see: McLeish, T C B “A Hitch-Hiker's Guide to Polymer Rheology”, *Rheol. Bull.*, 43 (2000) 8.
21. Kaya A, Cranfield College of Aeronautics Note no. 134 (1962).
22. Berstein B, Kearsley E A and Zapas L J, *Trans. Soc. Rheol.*, 7 (1963) 391.
23. McLeish T C B and Ball R C, *J. Polym. Sci. Polym., Phys. Edn*, 24 (1986) 1755; McLeish T C B, *J. Polym. Sci. Polym., Phys. Edn*, 25 (1987) 2253.
24. Watanabe H and Kotaka T, *Macromolecules*, 17 (1984) 2316.

25. Pearson D S and Halfand E, *Macromolecules*, 17 (1984) 888.
26. Brown E F and Burghardt W, *J. Rheol.*, 407 (1996) 37.
27. Kornfield J, Fuller G and Pearson D S, *Macromolecules*, 22 (1989) 1334.
28. Higgins J S and Roots J E, *J. Chem. Soc., Faraday Trans.*, 81 (1985) 757.
29. Richter D, Ewen B, Farago B and Wagner T, *Phys. Rev. Lett.*, 62 (1989) 2140.
30. Schleger P, Farago B, Lartigue C, Kollmar A and Richter D, *Phys. Rev. Lett.*, 81 (1998) 124.
31. Komlosch M E and Callaghan P T, *J. Chem., Phys.*, 109 (1998) 10053.
32. Klein P G, Adams C H, Brereton M G, Ries M E, Nicholson T M, Hutchings L R and Richards R W, *Macromolecules*, 31 (1998) 8871.
33. Kimmich R, Kopf M, and Callaghan P T, *J. Polym. Sci. B, Polym. Phys. Edn.*, 29 (1991) 1025.
34. Adams C H, Brereton M G, Hutchings L R, Klein P G, McLeish T C B, Richards R W and Ries M E, *Macromolecules*, 33 (2000) 7101.
35. Watanabe H., *Prog. Polym. Sci.*, 24 (1999) 1253.
36. Muller R, Pesce J J and Picot C, *Macromolecules*, 26 (1993) 4356.
37. McLeish T C B, Allgaier J, Bick D K, Bishko G, Biswas P, Blackwell R, Blottière B, Clarke N, Gibbs B, Groves D J, Hakiki A, Heenan R, Johnson J M, Kant R, Read D J and Young R N, *Macromolecules*, 32 (1999) 6734-6758.
38. Boué F, Nierlich M, Jannink G and Ball R C, *J. Phys. (France)*, 43 (1982) 137
39. Lodge T P, *Phys. Rev. Lett.*, 83 (1999) 3218.
40. Vlassopoulos D, Pakula T, Fytas G, Roovers J, Karatasos K and Hadjichristidis N, *Europhys. Lett.*, 39 (1997) 617.
41. Pütz M, Kremer K and Grest G S, *Europhys. Lett.*, 49 (2000) 735.
42. Skolnick J and Yaris R, *J. Chem. Phys.*, 881 (1988) 1418.
43. Everaers R, *Eur. Phys. J. B*, 4 (1998) 341.
44. McLeish T C B and Milner S T, *Adv. Polym. Sci.*, 143 (1998) 195.
45. Milner S T and McLeish T C B, *Phys. Rev. Lett.*, 81 (1998) 725.
46. Likhtman A E and McLeish T C B, *Macromolecules*, 35 (2002) 6332-6343.
47. Marrucci G, *J. Non-Newt. Fluid Mech.*, 62 (1996) 279.
48. Mead D W, Doi M and Larson R G, *Macromolecules*, 31 (1998) 7895.
49. Likhtman A E, McLeish T C B and Milner S T, *Phys. Rev. Lett.*, 85 (2000) 4550.
50. Ronca G, *J. Chem. Phys.*, 79 (1983) 1031.

51. Schweizer K S, Fuchs M, Szamel G, Guenza M and Tang H, *Macromol. Theory Simul.*, 6 (1997) 1037.
52. Hess W, *Macromolecules*, 19 (1986) 1395; Hess, W, *Macromolecules*, 20 (1987) 2589.
53. Pattamaprom C, Larson R G and Van Dyke T J, *Rheol. Acta.*, 39 (2000) 517.
54. Wagner M H and Schaeffer J, *Rheol. Acta.*, 33 (1994) 506.
55. Martin P C, Parodi G and Pershan P S, *Phys. Rev. A*, 6 (1972) 2401.
56. Öttinger H C, “*Stochastic Processes in Polymeric Fluids*”, Springer-Verlag (Berlin), (1996).
57. Leonardi F, Allal A and Marin G, *Rheol. Acta.*, 37 (1998) 199.
58. Thimm W, Friedrich C, Marth M and Honerkamp J, *J. Rheol.*, 43 (1999) 1663.
59. Thimm W, Friedrich C, Marth M and Honerkamp J, *J. Rheol.*, 44 (2000) 429.
60. Janzen J and Colby R H, *J. Mol. Structure*, 486 (1999) 569.
61. Read D J and McLeish T C B, *Macromolecules*, 34 (2001) 1928.
62. Wagner M H, Bastien H, Ehreckhe P, Kraft M, Hachmann P and Meissner J, *J. Non-Newt. Fluid Mech.* 79 (1998) 283.
63. Mhetar V R and Archer L A, *J. Non-Newt. Fluid Mech.*, 81 (1999) 71.
64. Marrucci G, Greco F and Ianniruberto G, *J. Rheol.*, 44 (2000) 845.
65. Morse D C, *Macromolecules*, 31 (1998) 7030.
66. Morse D C, *Macromolecules*, 31 (1998) 7044.
67. Fetters L J, Lohse D J and Graessley W W, *J. Polym. Sci., Polym. Phys. Edn.*, 37 (1999) 1023.
68. Fetters L J, Lohse D J, Milner S T and Graessley W W, *Macromolecules*, 32 (1999) 6847.
69. Prager S and Frisch H L, *J. Chem. Phys.*, 46 (1967) 1475.
70. Iwata K, *J. Chem. Phys.*, 76 (1982) 6363; *J. Chem. Phys.*, 83 (1985) 1969.
71. Iwata K and Edwards S F, *J. Chem. Phys.*, 90 (1989) 4567.
72. Brereton M G and Filbrandt M, *Polymer*, 26 (1986) 1134.
73. Müller-Needebock K K, McLeish T C B and Edwards S F, *J. Chem. Phys.*, 111 (1999) 8196-8208 .
74. Rubinstein M and Colby R H, *J. Chem. Phys.*, 89 (1988) 5291.
75. Vologodskii A V, Lukashin A V and Frank-Kamanetski M D, *Sov. Phys.—JETP*, 40 (1975) 932.
76. Kavassalis T A and Noolandi J, *Macromolecules*, 21 (1988) 2869.
77. Warner M and Edwards S F, *J. Phys. A*, 11 (1978) 1649.

78. Rubinstein M and Panyukov S, *Macromolecules*, 30 (1997) 8036.
79. Read D J and McLeish T C B, *Macromolecules*, 30 (1997) 6376.
80. Mergell B and Everaers R, *Macromolecules*, 34 (2001) 5675-5686.
81. Doi M and Kuzuu N Y, *J. Polym. Sci., Polym. Lett. Edn.*, 18 (1980) 775.
82. Marrucci G, *J. Polym. Sci. Polym. Phys. Edn.*, 23 (1985) 159.
83. Ball R C and McLeish T C B, *Macromolecules*, 22 (1989) 1911-1913.
84. Milner S T and McLeish T C B, *Macromolecules*, 30 (1997) 2159-2166.
85. Milner S T, McLeish T C B, Young R N, Hakiki A and Johnson J, *Macromolecules*, 31 (1998) 9345-9353.
86. Blottière B, McLeish T C B, Hakiki A, Young R N and Milner S T, *Macromolecules*, 31 (1998) 9295.
87. Daniels R, McLeish T C B, Crosby B J, Young R N and Ferneyhough C, *Macromolecules*, 34 (2001) 7025-7033.
88. Doi M and Edwards S F, “The Theory of Polymer Dynamics”, (Oxford), (1986)
89. Rubinstein M in “Theoretical Challenges in the Dynamics of Complex Fluids”, (Editor: T C B McLeish), Kluwer (Dordrecht), (1998).
90. Shull K R, Kramer E S and Fetters L J, *Nature*, 345 (1990) 790.
91. Viovy J L, Rubinstein M and Colby R H, *Macromolecules*, 24 (1991) 3587.
92. Frischknecht A L and Milner S T, *Macromolecules*, 33 (2000) 9764-9768 .
93. Watanabe H, Matsumiya Y and Inoue T, *Macromolecules*, 35 (2002) 2339-2357.
94. McLeish T C B, *J. Rheol.*, 47 (2003) (in press).
95. Meerkov S M and Runolfsson T, *IEEE Trans. Aut. Cont.*, 33 (1988) 323-332 .
96. Shanbhag S, Larson R G, Takimoto J and Doi M, *Phys. Rev. Lett.*, 87 (2001) 195502.
97. Frischknecht A L, Milner S T, Pryke R, Young R N, Hawkins R and McLeish T C B, *Macromolecules*, 35 (2002) 4801-4820.
98. Roovers J., *Macromolecules*, 18 (1985) 1359.
99. McKenna G B, et al, *Macromolecules*, 20 (1987) 498.
100. Roovers J, *Macromolecules*, 21 (1988) 1517.
101. Cates M E and Deutsch J M, *J. Phys. (Paris)*, 47 (1986) 2121.
102. Obhukov S P, Rubinstein M and Duke T, *Phys. Rev. Lett.*, 73 (1994) 1263.
103. Brown S, Lenczycki T and Szamel G, *Phys. Rev. E*, 63 (2001) 052801.
104. Bielawski C W, Benitez D and Grubbs R H, *Science*, (2002) 297.

105. Bercea M, Peiti C, Dimionescu B and Navard P, *Macromolecules*, 26 (1993) 7095.
106. Fischer E and Callaghan P T, *Phys. Rev. E*, 63 (2001) 6401.
107. Ianniruberto G and Marrucci G, *J. Non-Newt. Fluid. Mech.*, 65 (1996) 241.
108. Hua C C and Schieber J D, *J. Chem. Phys.*, 109 (1998) 10018; Hua C C and Schieber J D, *J. Chem. Phys.*, 109 (1998) 10028.
109. Milner S T, McLeish T C B and Likhtman A E, *J. Rheol.*, 45 (2001) 539.
110. Graham R S, Likhtman A E, Milner S T and McLeish T C B, *J. Rheol.*, 47 (2003) (submitted).
111. Read D J, *J. Rheol.*, 47 (2003) (submitted).
112. Menezes E V and Graessley W W, *J. Polym. Sci., Polym. Phys. Edn.*, 20 (1982) 1817.
113. Sridhar T, Oberhauser J, Leal G H, *J. Rheol.*, 47 (2003) (in press).
114. Likhtman A E, *J. Non-Newt. Fluid. Mech.*, 84 (2002) (submitted).